In vitro measurements of optical properties of porcine brain using a novel compact device

N. Yavari[1,2]   J. S. Dam[3]   J. Antonsson[4]   K. Wårdell[4]
S. Andersson-Engels[1]

[1]Department of Physics, Lund Institute of Technology, Lund, Sweden
[2]Department of Physics and Technology, University of Bergen, Bergen, Norway
[3]National Laser Centre, CSIR, Pretoria, South Africa
[4]Department of Biomedical Engineering, Linköping University, Sweden

Abstract—*Knowledge of the optical properties of tissues can be applied in numerous medical and scientific fields, including cancer diagnostics and therapy. There are many different ways of determining the optical properties of turbid media. The paper describes measurements of the optical properties of porcine brain tissue using novel instrumentation for simultaneous absorption and scattering characterisation of small turbid samples. Integrating sphere measurements are widely used as a reference method for determination of the optical properties of relatively thin turbid samples. However, this technique is associated with bulky equipment, complicated measuring techniques, interference compensation techniques and inconvenient sample handling. It is believed that the sphere for some applications can be replaced by a new, compact device, called the combined angular and spatially resolved head sensor, to measure the optical properties of thin turbid samples. The results compare very well with data obtained with an integrating sphere for well-defined samples. The instrument was shown to be accurate to within 12% for μ_a and 1% for μ_s' in measurements of intralipid-ink samples. The corresponding variations of data were 17% and 2%, respectively. The reduced scattering coefficient for porcine white matter was measured to be 100 cm^{-1} at 633 nm, and the value for coagulated brain tissue was 65 cm^{-1}. The corresponding absorption coefficients were 2 and 3 cm^{-1}, respectively.*

Keywords—*Optical properties, Turbid media, Integrating sphere, CASH sensor, Porcine brain tissue, Scattering*

1 Introduction

QUANTITATIVE INFORMATION on the concentration of the constituents of different turbid media, e.g. tissues, can be obtained by measuring the optical properties of the materials. The optical properties of a turbid medium, i.e. the absorption coefficient μ_a, the scattering properties (reduced scattering coefficient μ_s', or scattering coefficient, μ_s) and anisotropy factor g (WELCH and VAN GEMERT, 1995), can thus provide important information on the composition and the dynamics of a medium.

Whereas μ_a provides information on the concentration of various chromophores (JACQUES, 1996b), the scattering properties provide information on the form, size and concentration of the scattering components in the medium (JACQUES, 1996a; MOURANT et al., 1998). Thus accurate and fast determination of μ_a and the scattering properties of turbid media is useful and important in numerous fields of science and medicine, as well as in industry and environmental monitoring etc. In this study, we focused on biomedical applications and measurements of the optical properties of brain tissue.

In biomedicine, the distribution of light in tissue depends on the optical interaction coefficients and the illumination geometry. Knowledge of these coefficients is therefore essential for optically based diagnostic and therapeutic procedures (DRIVER et al., 1991; YAROSLAVSKY et al., 2002). Optical measurements of brain tissue have recently attracted much interest, especially for brain activation studies (BOAS et al., 2001; FRANCESCHINI et al., 2002; SCHROETER et al., 2004; WÅRDELL et al., 2004; WOLF et al., 2003) and for planning photodynamic therapy in the treatment of brain tumours (FRIESEN et al., 2002; MORIYAMA et al., 2004; SCHMIDT et al., 2004; STYLLI et al., 2004). Another area of interest is the assessment of lesion size and site during radio frequency (RF) ablation for the treatment of motor disorders caused, for example, by Parkinson's disease (ANTONSSON et al., 2005). In this paper, results are presented from optical measurements on normal and coagulated porcine brain tissue.

Measurements of the optical properties of tissue can be performed *in vivo* or *in vitro*. Most *in vivo* measurements performed to date rely on frequency-domain measurements

(FANTINI *et al.*, 1995), or time or spatially resolved measurements (CUBEDDU *et al.*, 1996; MADSEN *et al.*, 1992), utilising an inverse algorithm to extract the optical properties. This algorithm is usually based on the diffusion approximation and the fact that the tissue is relatively homogeneous within a relatively large probe volume. These requirements are not always completely fulfilled, and the techniques used in such cases are thus limited to providing relative rather than absolute values, such as spatial or temporal variations in the optical properties.

Novel techniques to measure absorption and scattering spectra in a much smaller probe volume have been suggested (AMELINK *et al.*, 2004; AMELINK and STERENBERG, 2004; BIGIO and BOWN, 2004; JOHNSON *et al.*, 2004; MOURANT *et al.*, 1999). A disadvantage of these techniques is that they cannot accurately measure small absorption coefficients, as characteristic for tissue in this wavelength region. The most frequently used method of measuring the optical properties of small tissue volumes is the integrating sphere (IS), which is used to probe a thin slice of excised tissue (PICKERING *et al.*, 1992). This can be used as either a three-parameter technique for extracting μ_a, μ_s, and g from measured total diffused reflectance R_{tot}, total diffused transmittance T_{tot} and collimated transmittance T_{col}, or as a two-parameter technique for measuring μ_a and μ_s' from the recorded values of R_{tot} and T_{tot}.

The technique has been shown to provide relatively accurate results for tissue phantoms (DAM *et al.*, 2000). However, it is debatable how the optical properties are affected by tissue excision and sample preparation. Also, the sample thickness most suitable to obtain an optimum signal-to-noise ratio in the evaluation differs for R_{tot}, T_{tot} and T_{col}. Therefore a compromise must be made, and a thickness that is reasonably suitable for all measurements has to be used. This usually results in a poor signal-to-noise ratio in the measured value of T_{col}. In addition, bulky instrumentation and sample handling make the measurements complicated.

To circumvent some of these problems, we have developed a novel system for measuring the optical properties of tissue, presented by DAM *et al.* (2005). This system is constructed to enable real-time, simultaneous determination of μ_a, μ_s, and g from thin turbid samples using a continuous wave (i.e. steady-state) light source. In this study, we focused on measuring the absorption and reduced scattering coefficients (μ_a and μ_s'), using both the new system and an IS as a reference system. To extract these coefficients in the new system, we measured the spatially resolved diffuse reflectance R and angularly resolved diffuse transmittance α. Both the IS system and the new sensor were calibrated and optimised for the measurements using suspensions of intralipid and ink. Intralipid is a fat emulsion that is used clinically as an intravenously administered nutrient and, in research, provides the scattering component in a tissue phantom to investigate the propagation of light in tissue (VAN STAVEREN *et al.*, 1991).

The aims of this work were to measure the optical properties of porcine brain tissue before and after coagulation with a monopolar radio-frequency electrode and to evaluate whether our newly developed instrument could provide accurate results for real tissue measurements.

2 Materials and methods

2.1 *CASH sensor measurements*

The combined angular and spatially resolved head (CASH) sensor is a new compact device that may prove to be a good alternative to the integrating sphere system. The device, designed and constructed in collaboration between Bang
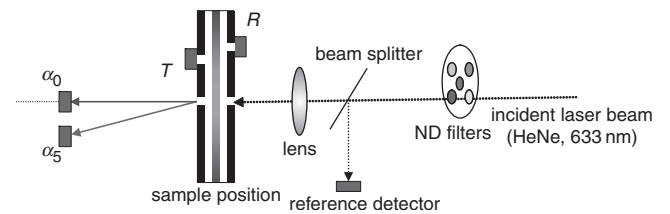
Fig. 1 *CASH sensor set-up. R, T, α_0 and α_5 denote light referred to as reflectance, transmittance, and angular transmittance at $0°$ and $5°$ to detectors, respectively. Light is collected by optical fibres. Neutral density (ND) filters were used to increase dynamic range of measurements*

& Olufsen Medicom A/S, Denmark, and the Department of Physics, Lund University, is illustrated in Fig. 1.

A 2 mW HeNe laser (633 nm) with a beam diameter of 1.0 mm was used as a light source. Part of the beam was split off to a reference detector to check that the output from the laser remained constant throughout the measurements. The rest of the light beam was aligned and sufficiently focused to pass through a hole ($\phi = 1.0$ mm) in a black metal sheet to irradiate the central part of the cuvette. The cuvette was mounted between two black metal sheets. In the centre of the cuvette, transmitted light could escape through a 1.0 mm diameter hole. Two 400 μm core diameter optical fibres were placed at a distance of 75 mm from the cuvette surface to collect light escaping at two angles of $0°$ and $5°$, the signals being denoted α_0 and α_5, respectively. The flat polished ends of two other 400 μm fibres were mounted in holes next to the cuvette at radial distances of 2.5 mm (R) and 2.0 mm (T). Only the α_0 and R signals were used in the subsequent analysis, as we only aimed to extract μ_a and μ_s'. The optical fibres were terminated on Si detectors controlled by a Labview PC card. The detectors were used to read the light intensities from each fibre. All signals were recorded simultaneously using an exposure time of 10 ms.

2.2 *Integrating sphere measurements*

In Fig. 2, the arrangement used for the IS method is illustrated (DAM *et al.*, 2000; NILSSON *et al.*, 1998). A 75 W Xe lamp is coupled into one 600 μm fibre, providing light in a broad spectral region. The light is formed into a ~2 mm parallel light beam using a positive lens with a 10 mm focal length. If the sample is placed at position A or B, the transmitted and the diffusely reflected light flux, I_T and I_R, respectively, can be acquired (SWARTLING *et al.*, 2003b). The light was spectrally dispersed in a spectrometer[*] with a 150 grooves mm^{-1} grating. A liquid nitrogen cooled CCD camera[†] connected to the spectrometer was used to capture the spectra. The data were subsequently transferred to a computer for storage and analysis.

The total reflectance R_{tot} and transmittance T_{tot} were obtained from the measured data by applying the following equations:

$$R_{tot} = R_{BS} \cdot \frac{I_R}{I_{ref}} \tag{1}$$

$$T_{tot} = \frac{I_T}{I_{ref}} \tag{2}$$

where I_R is the measured intensity of the reflectance flux with the sample at position B; I_T is the measured intensity of the transmittance with the sample at position A and a barium

---

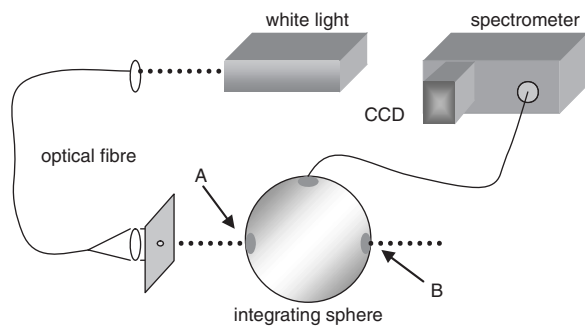[*]270 M, SPEX Industries Inc.
[†]EG&G

Fig. 2 *Integrating sphere set-up. A and B are sample positions for measurements of T and R, respectively*

sulphate plug (standard sample) at position B; and I_{ref} is the reference signal with the standard sample placed at position B. The barium sulphate plug is a calibration standard with a certified reflectance factor, R_{BS}.

2.3 Samples and sample preparation

To calibrate both the systems, liquid samples containing a mixture of intralipid, ink and water were prepared in ten groups. Each group contained ten samples with fixed intralipid concentration, providing a constant scattering coefficient, and the concentration of ink was varied in between 0.001 and 0.1% to provide ten different absorption coefficients. Likewise, the intralipid concentration was varied between groups within the range 0.4–6.8% to provide ten different scattering coefficients. In this way a matrix of samples was formed with optical properties covering the typical biological range of absorption and scattering coefficients

$$0.1\,\text{cm}^{-1} \leqslant \mu_a < 10\,\text{cm}^{-1}$$
$$5\,\text{cm}^{-1} \leqslant \mu_s' < 85\,\text{cm}^{-1}$$

Identical cuvettes were made for the measurements, consisting of two glass microscope slides (1 mm thickness) glued with an air gap of 0.3 mm between them. One end was left open so that the liquid sample could be introduced.

This study of the optical properties of brain tissue is part of a larger study approved by the local Ethical Committee for animal research (Project 42-01, Linköping University). Brain tissue samples were taken from five Swedish native-bred pigs with a body weight of 20.5 kg $\pm$ 0.5 kg. After premedication and general anaesthesia, a stereotactic frame with modified posts[‡] was attached to the pig's skull. Magnetic resonance (MR) images were taken before surgery so that the target areas located in the thalamic region could be identified. The procedure corresponds to bilateral thalamotomy in human neurosurgery. The target and entering co-ordinates were determined from the MR images by an experienced neuroradiologist.

Two 3 mm burr holes, 3 cm apart, were drilled in the skull, and a monopolar radio frequency coagulating electrode (2 mm in diameter) was inserted into the brain tissue and guided along the planned trajectory. A lesion was produced in the predefined target area with temperature settings from 70 to 90°C during a period of 60 s. A neuro generator power supply was used.[**] After surgery, the pigs were sacrificed with an overdose of barbiturates, administered intravenously and intracardially.

The coagulated tissue was removed with a specially designed punch within 2 h of death and stored at −20°C in a freezer. Five white matter and five coagulated lesion samples

---

[‡]G frame, Elekta Instruments AB, Sweden
[**]Leksell, model LNG 30-1, Elekta instruments AB, Sweden

were prepared and investigated with the optical systems. These samples were taken from the freezer just prior to the measurements and prepared at room temperature. Small slices were cut to a thickness of 0.3 mm, 2 cm in diameter. These slices were placed between two glass plates with 0.3 mm spacers at each side for measurements. The glass slides were marked to ensure that the same part of each sample was irradiated in all the measurements. The optical measurements were performed within 3 h of thawing. During this time, the samples were stored at room temperature, wrapped in thin plastic film.

2.4 Measurement procedure

The intralipid–ink samples were used in ten sets of ten samples, prepared as described above, to calibrate and evaluate the performance of both systems. The 0.3 mm thick cuvettes were first filled with samples 1–10 from group one. For IS measurements, all ports on the IS were first blocked so that the background could be recorded. For the IS measurements, a standardised acquisition time of 10 s was employed. Then, while port B was still blocked, we recorded the reference intensity I_{ref} of the lamp through port A of the sphere. Next, with port B still blocked, one of the cuvettes was placed at port A to record the transmission of light through the sample (I_T). After this recording, the cuvette was repositioned at port B, where the reflected light from the sample could be measured (I_R). For this measurement, port A was kept open.

Following these recordings, measurements were conducted with the CASH sensor. First the background was recorded with all detectors by blocking the laser light, followed by a laser intensity measurement by the reference detector. The laser light was then attenuated with a neutral density filter[††] (1.0 mm), and the intensity at the α_0 detector was recorded to ensure the stability of the system. The cuvettes were then placed in the cuvette holder, one by one, for the recordings. All samples were measured both with and without different combinations of neutral density filters to improve the dynamic range of detection. The acquisition time for each measurement was 10 ms. Following measurements on all the samples in one group, the cuvettes were washed with distilled water and filled with the samples from the next group. Measurements on the pig brain samples were performed following the same procedure, except that several measurements were performed at different positions on each sample with the CASH sensor.

2.5 Data processing

The problem of extracting the optical properties from measured data is multidimensional. The optical properties were obtained from measurements in three steps, as described below. Basically, a multiple polynomial regression (MPR) technique was used, employing fitting of an analytical expression to a discrete number of measured or modelled data points (DAM *et al.*, 2000). In this way, a simple expression was obtained describing the behaviour of the measured parameters as a function of the optical properties. This provides a fast and accurate method for applications involving real-time, multiparameter extraction problems. Rapid data processing is of particular importance for spectral recordings including data from a large number of wavelengths. The MPR method was utilised to calibrate and evaluate measurements from both the IS system and the CASH sensor.

The MPR method was used to extract μ_a and μ_s' from IS measurements of R_{tot} and T_{tot} on thin turbid samples. In MPR, the first step (calibration) is to perform two objective

---

[††]NG1, Schott, Germany

mappings of relevant subsets of the $[\mu_a, \mu'_s]$ space onto their images in R_{tot} and T_{tot} space, respectively. Monte Carlo simulations using the code provided by WANG and JACQUES (1992) were employed for this purpose. The R_{tot} and T_{tot} values were simulated for a 38×38 matrix of μ_a and μ'_s. The values in these matrices were chosen so that their distributions were wider than their typical biological ranges (BEEK *et al.*, 1997; CHEONG *et al.*, 1990)

$$0.01 \, \text{cm}^{-1} \leqslant \mu_a \leqslant 10 \, \text{cm}^{-1}$$
$$3 \, \text{cm}^{-1} \leqslant \mu'_s \leqslant 500 \, \text{cm}^{-1}$$
$$g = 0.74$$
$$n = 1.33$$

The anisotropy factor g and the refractive index n were kept fixed in the simulations. The geometry of the sample in the simulation was a semi-infinite slice of 0.3 mm thickness. The slice was placed between two glass slides with a thickness of 1 mm, and $n = 1.5$. The beam diameter was set at 2 mm, and the acceptance hole of the ports to the integrating sphere was set at 25 mm. In each simulation, 1×10^5 photons were traced.

The second step (fitting) involves creating a calibration model describing $R_{tot} (\mu_a, \mu'_s)$ and $T_{tot} (\mu_a, \mu'_s)$ by polynomial regression. Here, a fifth degree polynomial was used for both μ_a and μ'_s.

Finally, in the last step (evaluation), the Newton–Raphson algorithm was applied to extract μ_a and μ'_s from IS measurements of R_{tot} and T_{tot} by solving the inverse problem. This was performed both for the intralipid–ink samples and brain tissue samples. Evaluations were conducted for all wavelengths between 520 and 770 nm.

The CASH sensor was also calibrated and evaluated using the MPR technique. In this case, we chose to limit the evaluation to two measured properties, R and α_0. The database was generated from values measured in the intralipid–ink samples with known values of μ_a and μ'_s (VAN STAVEREN *et al.*, 1991). In this way, we generated 10×10 matrices for R and α_0. The values of μ_a and μ'_s in these matrices were chosen to be somewhat wider than their typical biological ranges

$$0.1 \, \text{cm}^{-1} \leqslant \mu_a < 10 \, \text{cm}^{-1}$$
$$5 \, \text{cm}^{-1} \leqslant \mu'_s < 85 \, \text{cm}^{-1}$$
$$g = 0.74$$
$$n = 1.33$$

3 Results

Fig. 3 shows the simulated functions $R_{tot} (\mu_a, \mu'_s)$ and $T_{tot} (\mu_a, \mu'_s)$, obtained from Monte Carlo simulations for the integrated sphere, and the fitted $R_{tot} (\mu_a, \mu'_s)$ and $T_{tot} (\mu_a, \mu'_s)$ functions using multiple polynomial regression.

The relative errors in $R_{tot} (\mu_a, \mu'_s)$ and $T_{tot} (\mu_a, \mu'_s)$ obtained in the fit to the Monte Carlo generated data are shown in Fig. 4.

Fig. 5 shows measured values of R and α_0 using intralipid–ink samples and the corresponding fitted values for the CASH sensor. The relative error between the fitted polynomial (MPR) and the database (measured values) in R and α_0 is shown in Fig. 6. The fit is considerably noisier than for the integrating sphere calibration, indicating a lower signal-to-noise ratio in the data used for the fits.

Before using the systems for measurements on tissue, we determined how accurately and precisely the optical properties could be extracted from the two systems. For this, we used the measurements on the intralipid–ink samples with known
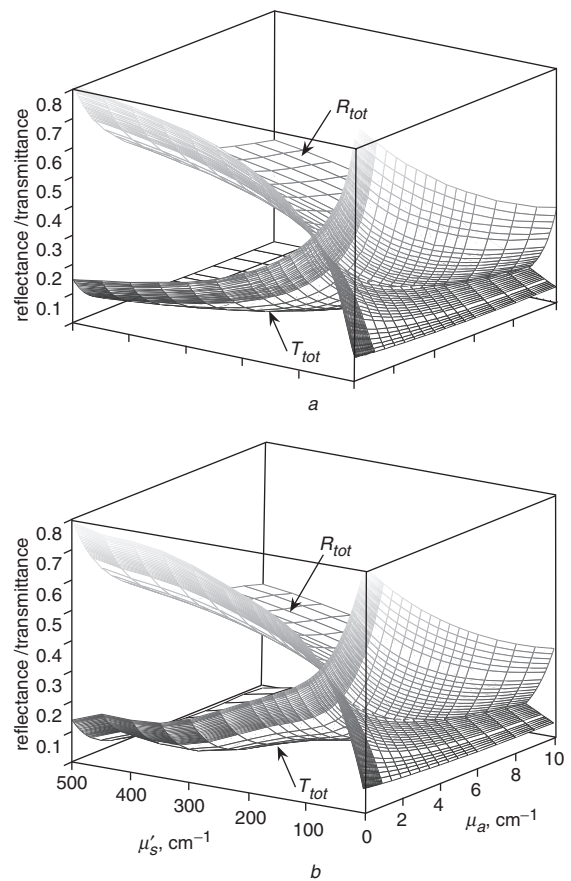
Fig. 3 *Reflectance and transmittance as function of absorption coefficient μ_a and reduced scattering coefficient μ'_s for thin slice geometry. R_{tot} and T_{tot} were generated with (a) Monte Carlo simulation, (b) MPR*
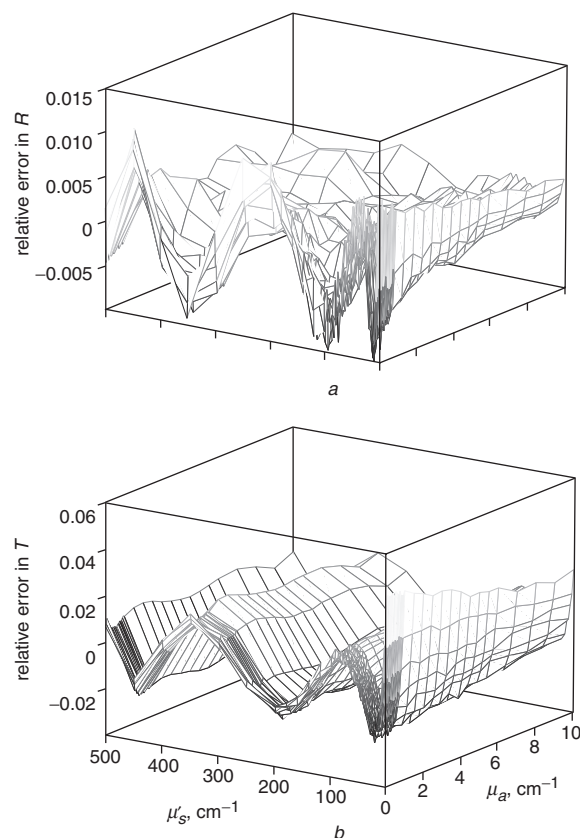

Fig. 4 *Relative error between Monte Carlo simulated data and MPR data, for (a) total reflectance and (b) total transmittance*
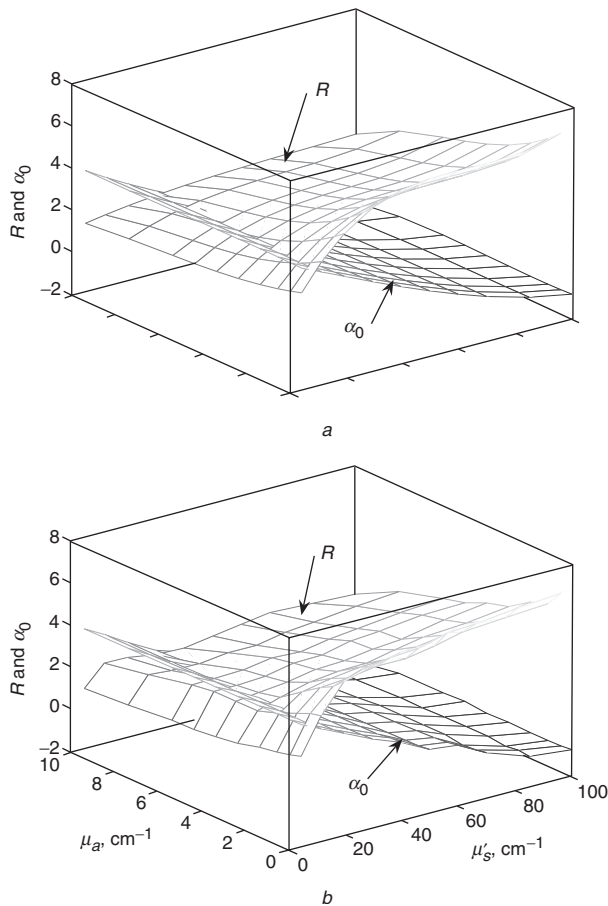
Fig. 5 *(a) Fitted polynomials for R and α_0, and (b) measured values of R and α_0*

Fig. 6 *Relative error between measured values and MPR data, for (a) R and (b) α_0*

optical properties. Fifty samples were used for a temporary calibration, and the remaining 40 were used for evaluation of performance. As one of the aims of this study was to compare the IS and CASH sensor systems, data at 633 nm were selected for the IS system. Fig. 7 shows the values of μ_a and μ'_s of the intralipid–ink samples used for evaluation, measured with the IS and CASH sensor.

The precision and accuracy of the systems were quantified from these data. The inaccuracy was calculated according to (3), and the spread in data, given as the coefficient of variation (CV), was calculated using (4). The results are presented in Table 1, together with known optical properties obtained from the known concentrations of intralipid and ink.

$$\text{inaccuracy} = \frac{<x> - known(x)}{known(x)} \tag{3}$$

$$\text{CV} = \frac{\sigma(x)}{<x>} \tag{4}$$

where x refers to μ_a or μ'_s, $<x>$ refers to the mean value of the measured values of μ_a or μ'_s, and $\sigma(x)$ is the standard deviation of each set of μ_a and μ'_s.

After completing the evaluation of the systems, we performed measurements on the brain tissue samples from pigs. Results from IS measurements are presented in Fig. 8. Both absorption and scattering exhibit considerable variations in spectral shape between the two kinds of sample. Also, crosstalk between the absorption and scattering is visible around the haemoglobin peaks in the spectra, as the scattering spectra are supposed to be structureless. The influence of this
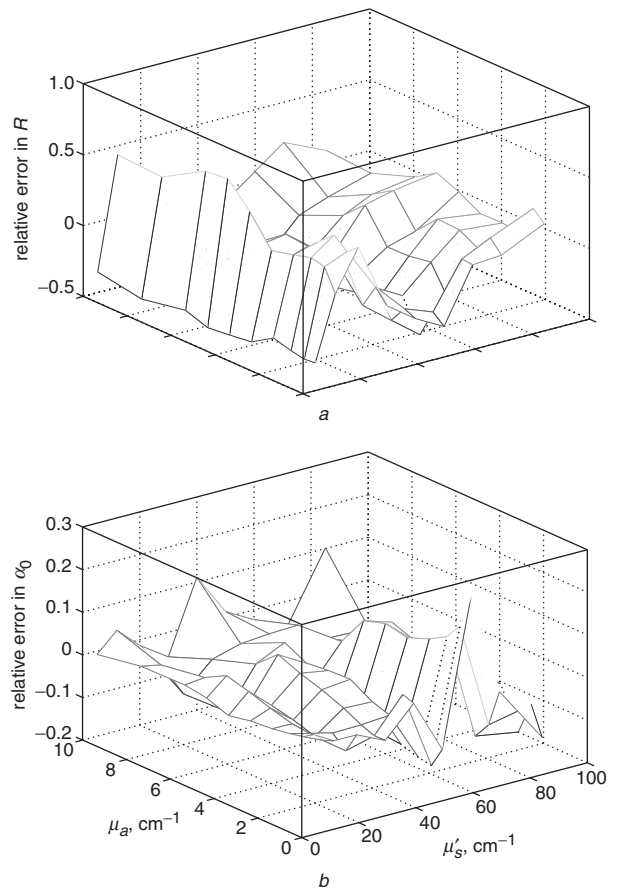
cross talk falls, however, within the limits of measured accuracy of the technique.

As the CASH sensor measures the light scattered from a considerably smaller volume, measurements could be performed on smaller, visually more homogeneous, regions of the samples, and several measurements could be performed at different positions in the same sample. The CASH sensor provided very reproducible results, and results from different measurements on the same sample but at slightly different positions gave a CV of 8% for μ'_s and 15% for μ_a in normal white matter; and 4% for μ'_s and 17% for μ_a in coagulated brain tissue. All measurements on a single sample with the CASH sensor were recorded from visually similar tissue. The variations in μ'_s are thus much higher than the variations in homogenous intralipid–ink samples, whereas the variations in μ_a already are quite high in these samples, and no difference could be observed for the brain samples. Results for absorption and scattering at 633 nm are presented in Figs 9 and 10 for white matter and coagulated brain tissue, respectively. The reference values in the Figures are derived from measurements on human brain tissue performed by YAROSLAVSKY *et al.* (2002).

4 Discussion and conclusions

In this work, we have introduced a novel technique for the determination of the optical properties of turbid media from spatially and angularly resolved measurements on a small, thin sample, i.e. a solid slice or liquid sample in a cuvette, using simple, continuous-wave, non-coherent light sources. The compact instrument developed allows rapid measurements
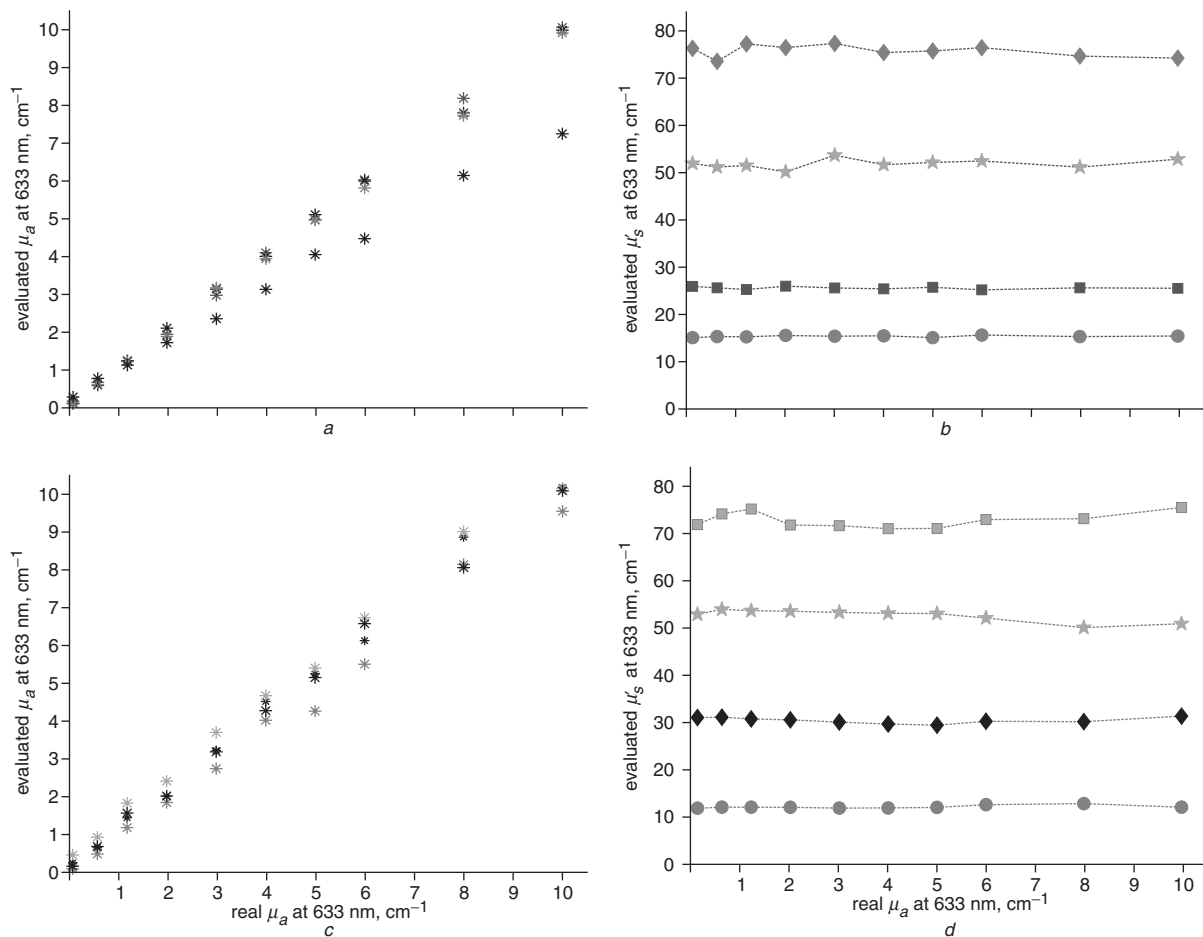
Fig. 7 *Absorption (μ_a) and reduced scattering coefficient (μ'_s) of intralipid–ink samples measured with (a), (b) IS and (c), (d) CASH sensor*

without repositioning of the sample, providing the possibility of real-time determination of optical properties. The acquisition time in this study was only 10 ms. This may be of special interest for certain measurements of liquids in process or food industries.

In this study, we have used the instruments to measure brain tissue samples. All results and conclusions presented are based on calibrations obtained from Monte Carlo simulation or real measurements using especially prepared liquid samples of known optical properties. As the presented results show, there is a very good correlation between the expected and the experimental results for these samples. In the evaluation of the system, the results for scattering agreed especially well with the expected values. The absorption varied more, probably owing to the small sampling volume, leading to low sensitivity to absorption in a medium with a relatively low absorption coefficient. In the measurements of brain tissue, the same training set was used. A small error is then introduced, as the g-factor is expected to be different for these samples. In a previous study, we have shown that a variation of g between 0.8 and 0.99 resulted in a $\pm 2.5\%$ error in the evaluated reduced scattering coefficient (DAM *et al.*, 2000). We thus

believe that we can neglect the effect of an assumed error in the g-factor used in the training set in the present study.

The evaluated new technique is interesting owing to the advantages it has over the IS method: the sample does not have to be moved during the measurements, no bulky spheres are needed, and there is the possibility of sampling smaller volumes (DAM *et al.*, 2005). As configured here, the CASH sensor obtains data at one wavelength only, whereas the IS system records full spectral information.

It is interesting to note that both systems yield a lower accuracy and CV for the reduced scattering, compared with the absorption coefficient. This is probably owing to the small sampling distance of the light within the tissue, resulting in a low probability of absorption. It is therefore difficult to evaluate the absorption property with high precision. This has been discussed in the past, see, for example, SWARTLING *et al.* (2003*a*).

The results from the liquid sample measurements were promising for the new sensor, and we thus continued with real tissue measurements. The results from these measurements show much larger variations between the samples than for the liquid samples used in the evaluation of the system. The variations observed from the tissue measurements are thus not believed to be due to insensitivity of the system, but rather due to variations between the samples. This is also suggested by the low variations observed within the same sample (data not shown) and because results from the IS set-up varied more than those for the CASH sensor. These small scale variations within tissue may complicate any diagnostic technique based on optical spectroscopy.

A probable explanation of these variations is the heterogeneity of brain tissue. In these measurements, it was sometimes
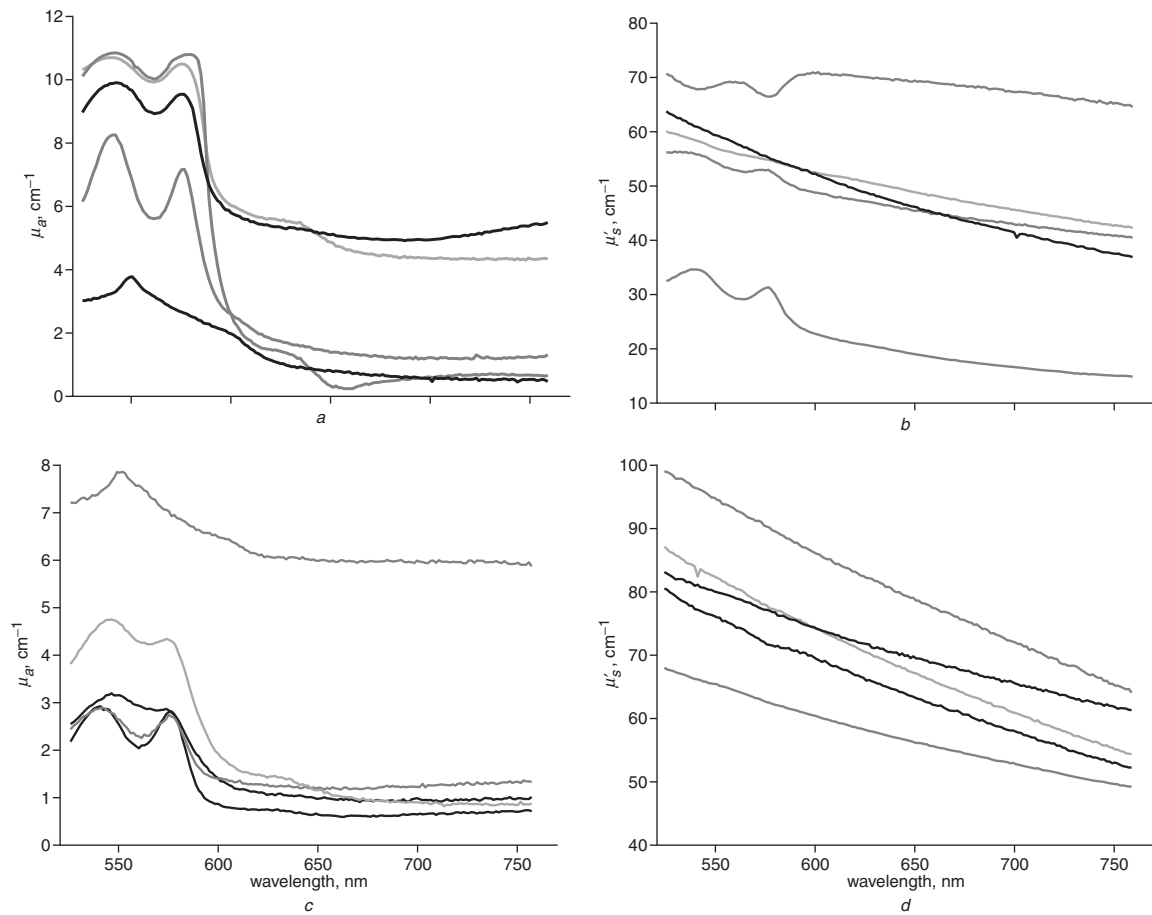
Table 1 Estimated inaccuracy and coefficient of variation of μ'_s and μ_a measurements of intralipid–ink samples, with IS and CASH sensor

Instrument	Inaccuracy, %		CV, %	
	μ_a	μ'_s	μ_a	μ'_s
Integrating sphere	9	7	6	1
CASH sensor	12	1	17	2

Fig. 8   *Evaluated spectra of porcine brain samples from five animals measured with integrating sphere set-up. (a) μ_a and (b) μ_s' measurements of coagulated tissue; (c) μ_a and (d) μ_s' measurements of white matter*
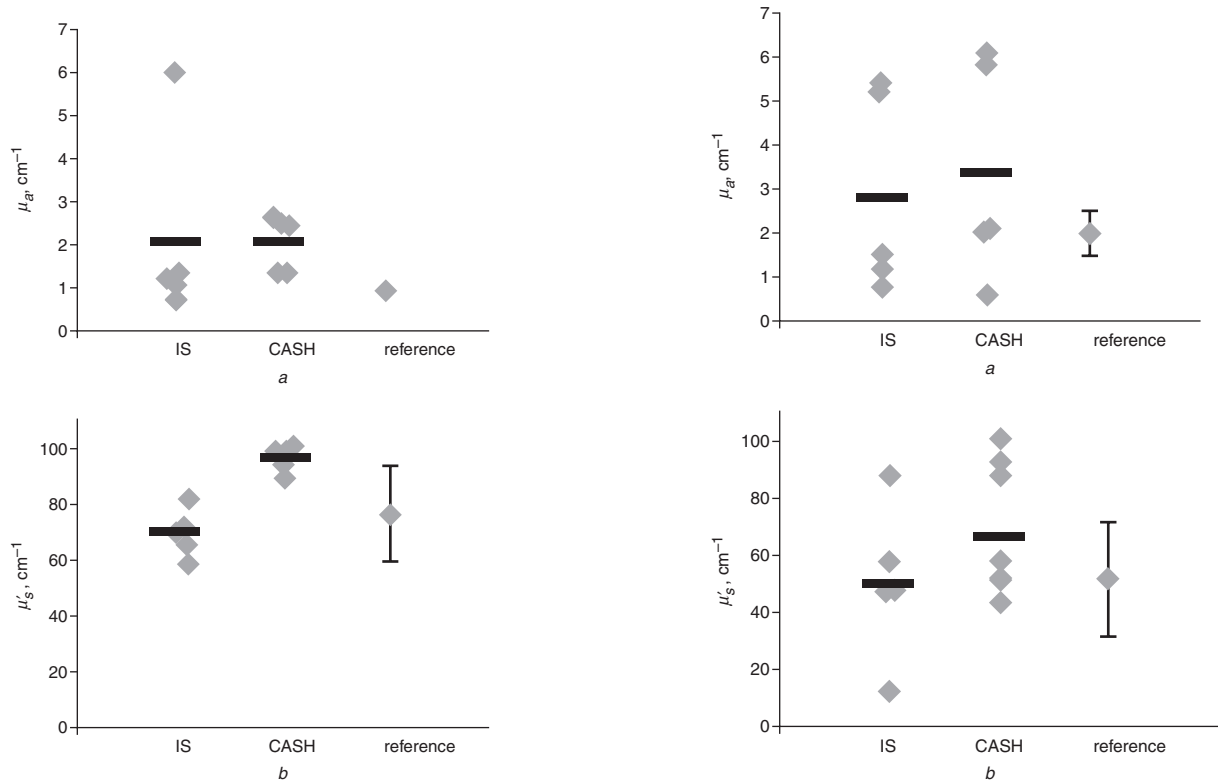

Fig. 9   *Results from measurements on white matter at 633 nm performed with IS and CASH sensor. Published data for human brain are denoted reference (error bars indicate variation of results obtained in published data; these variations are not visible in 9(a)). (a) Absorption coefficient measurements; (b) reduced scattering coefficient measurements*

Fig. 10   *Results from measurements on coagulated pig brain tissue at 633 nm performed with IS and CASH sensor. Published data for human brain are denoted reference (error bars indicate variation of results obtained in published data). (a) Absorption coefficient measurements, (b) reduced scattering coefficient measurements*

difficult to measure white matter or coagulated tissue only, as light was collected out to a distance of 12 mm from the optical axis in the IS set-up. This was sometimes sufficiently large to cover, not only the targeted tissue, but also other parts of the samples, areas not intended to be included in the measurement. It is thus important to conduct local measurements of optical properties, as brain tissue is very heterogeneous. The CASH sensor could be considerably better than the IS in this respect, as the probed volume is smaller. For this sensor, only light at a radius of 2.5 mm is detected. Measurements of neighbouring areas within the same brain tissue sample, using this sensor, also produced values within 5% of each other (data not shown). Interestingly, the optical properties for the coagulated brain tissue varied considerably more than those for the normal white matter. This could be owing to pieces of white matter intermixed with grey matter inside the coagulated volume. The targeted area for coagulation was always grey matter. Other factors that could cause variations in measured results are slight variations in sample preparation, sample thickness, sample positioning etc.

It is known that, in measurements on very thin samples, such as those in our experiments, tissue preparation affects the measured optical properties. It is mainly the absorption coefficient that is believed to alter, owing to loss of liquid constituents in tissue. For example, it has been shown that the effective light attenuation of tissue can change by a factor of two or more in the visible wavelength range where blood is the main absorber (FLOCK *et al.*, 1987; WILSON *et al.*, 1985). Also, the transmission of light through tissue can be altered by freezing and thawing (FLOCK *et al.*, 1987). The structural changes resulting from freezing and the reduction in tissue water content upon thawing affect the optical response of tissue. Changes of 39% and 160% in the transmission of a thick sample at 488 and 514 nm, respectively, due to prefreezing, have previously been reported (CHEONG *et al.*, 1990). This suggests loss of haemoglobin as a result of the freezing, and the effect is therefore most probably dependent on exactly how the samples are frozen. Also, it has been demonstrated that the optical properties measured from thick samples are generally smaller than those measured from thin samples (CHEONG, 1995).

These observations suggest that we should be aware of these problems, especially in evaluation of the absorption coefficient of tissue from *ex vivo* measurements. In these experiments, the samples were snap frozen in liquid nitrogen and kept frozen until the measurements. The samples were stored in relatively large chunks (several centimetres in diameter) and thawed wrapped in plastic foil to minimise the effects of loss of liquid. The samples were sliced just prior to the measurements, again to minimise alterations in the optical properties due to the sample preparation. The results from brain sample measurements are in good agreement with previous *ex vivo* observations (YAROSLAVSKY *et al.*, 2002). These values need to be reconfirmed by *in vivo* measurements.

Knowledge of the optical properties of normal and coagulated brain tissue is of great importance, especially for improving devices used in minimally invasive intervention and target localisation during stereotactic neurosurgery. There exists a large amount of research into the treatment of motor disorders such as Parkinson's disease. With new knowledge, it might be possible to perform surgery more safely and with higher accuracy in the future.

References

AMELINK, A., and STERENBORG, H. J. (2004): 'Measurement of the local optical properties of turbid media by differential path-length spectroscopy', *Appl. Opt.*, **43**, pp. 3048–3054

AMELINK, A., STERENBORG, H. J., BARD, M. P., and BURGERS, S. A. (2004): '*In vivo* measurement of the local optical properties of tissue by use of differential path-length spectroscopy', *Opt Lett.*, **29**, pp. 1087–1089

ANTONSSON, J., ERIKSSON, O., and WÅRDELL, K. (2005): '*In-vivo* reflection spectroscopy measurements in pig brain during stereotactic surgery', *SPIE*, pp. 242–250

BEEK, J. F., BLOKLAND, P., POSTHUMUS, P., AALDERS, M., PICKERING, J. W., STERENBORG, H. J. C. M., and VAN GEMERT, M. J. C. (1997): '*In vitro* double-integrating-sphere optical properties of tissues between 630 and 1064 nm', *Phys. Med. Biol.*, **42**, pp. 2255–2261

BIGIO, I. J., and BOWN, S. G. (2004): 'Spectroscopic sensing of cancer and cancer therapy: current status of translational research', *Cancer Biol Ther.*, **3**, pp. 259–267

BOAS, D. A., GAUDETTE, T., STRANGMAN, G., CHENG, X. F., MAROTA, J. J. A., and MANDEVILLE, J. B. (2001): 'The accuracy of near infrared spectroscopy and imaging during focal changes in cerebral hemodynamics', *Neuroimage*, **13**, pp. 76–90

CHEONG, W.-F., PRAHL, S. A., and WELCH, A. J. (1990): 'A review of the optical properties of biological tissues', *IEEE J. Quant. Electr.*, **26**, pp. 2166–2185

CHEONG, W.-F. (1995): 'Summary of optical properties', in WELCH, A. J., and VAN GEMERT, M. J. C. (Eds): 'optical-thermal response of laser-irradiated tissue', (Plenum Press, New York, 1995), pp. 275–303

CUBEDDU, R., PIFFERI, A., TARONI, P., TORRICELLI, A., and VALENTINI, G. (1996): 'Experimental test of theoretical models for time-resolved reflectance', *Med. Phys.*, **23**, pp. 1625–1633

DAM, J. S., DALGAARD, T., FABRICIUS, P. E., and ANDERSSON-ENGELS, S. (2000): 'Multiple polynomial regression method for determination of biomedical optical properties from integrating sphere measurements', *Appl. Opt.*, **39**, pp. 1202–1209

DAM, J. S., YAVARI, N., and ANDERSSON-ENGELS, S. (2005): 'Real-time absorption and scattering characterization of slab-shaped turbid samples using a combination of angular and spatially resolved measurements', *Appl. Opt.*, **44**, pp. 4281–4290

DRIVER, I., LOWDELL, C. P., and ASH, D. V. (1991): '*In vivo* measurement of the optical interaction coefficients of human tumours at 630 nm', *Phys. Med. Biol.*, **36**, pp. 805–813

FANTINI, S., FRANCESCHINI-FANTINI, M. A., MAIER, J. S., WALKER, S. A., BARBIERI, B., and GRATTON, E. (1995): 'Frequency-domain multichannel optical detector for noninvasive tissue spectroscopy and oximetry', *Opt. Eng.*, **34**, pp. 32–42

FLOCK, S. T., WILSON, B. C., and PATTERSON, M. S. (1987): 'Total attenuation coefficients and scattering phase functions of tissues and phantom materials at 633 nm', *Med. Phys.*, **14**, pp. 835–841

FRANCESCHINI, M. A., THOMPSON, J., CULVER, J. P., STRANGMAN, G., and BOAS, D. A. (2002): 'Looking for the fast signal: Neuronal and hemodynamic evoked responses of the sensory-motor cortex'. OSA Biomedical Topical Meetings, OSA Technical Digest, *OSA*, pp. 208–210

FRIESEN, S. A., HJORTLAND, G. O., MADSEN, S. J., HIRSCHBERG, H., ENGEBRATEN, O., NESLAND, J. M., and PENG, Q. (2002): '5-Amino-levulinic acid-based photodynamic detection and therapy of brain tumors (review)', *Int. J. Oncol.*, **21**, pp. 577–582

JACQUES, S. L. (1996a): 'Origins of tissue optical properties in the UVA, visible, and NIR regions', *Proc. OSA*, **2**, pp. 364–369

JACQUES, S. L. (1996b): 'Reflectance spectroscopy with optical fiber devices, and transcutaneous bilirubinometers', in VERGA SCHEGGI, A. M. *et al.* (Eds): 'Biomedical optical instrumentation and laser-assisted biotechnology, vol. 325' (Kluwer Academic Publishers, Dordrecht, 1996), pp. 83–94

JOHNSON, K. S., CHICKEN, D. W., PICKARD, D. C., LEE, A. C., BRIGGS, G., FALZON, M., BIGIO, I. J., KESHTGAR, M. R., and BOWN, S. G. (2004): 'Elastic scattering spectroscopy for intraoperative determination of sentinel lymph node status in the breast', *J Biomed Opt.*, **9**, pp. 1122–1128

MADSEN, S. J., WILSON, B. C., PATTERSON, M. S., PARK, Y. D., JACQUES, S. L., and HEFETZ, Y. (1992): 'Experimental tests of a simple diffusion model for the estimation of scattering and absorption coefficients of turbid media from time-resolved diffuse reflectance measure', *Appl. Opt.*, **31**, pp. 3509–3517

MORIYAMA, E. H., BISLAND, S. K., LILGE, L., and WILSON, B. C. (2004): 'Bioluminescence imaging of the response of rat gliosarcoma to ALA-PpIX-mediated photodynamic therapy', *Photochem. Photobiol.*, **80**, pp. 242–249

MOURANT, J. R., FREYER, J. P., HIELSCHER, A. H., EICK, A. A., SHEN, D., and JOHNSON, T. M. (1998): 'Mechanisms of light scattering from biological cells relevant to noninvasive optical-tissue diagnostics', *Appl. Opt.*, **37**, pp. 3586–3593

MOURANT, J. R., JOHNSON, T. M., LOS, G., and BIGIO, I. J. (1999): 'Non-invasive measurement of chemotherapy drug concentrations in tissue: preliminary demonstrations of in vivo measurements', *Phys. Med. Biol.*, **44**, pp. 1397–1417

NILSSON, A. M. K., STURESSON, C., LIU, D. L., and ANDERSSON-ENGELS, S. (1998): 'Changes in spectral shape of tissue optical properties in conjunction with laser-induced thermotherapy', *Appl. Opt.*, **37**, pp. 1256–1267

PICKERING, J. W., MOES, C. J. M., STERENBORG, H. J. C. M., PRAHL, S. A., and VAN GEMERT, M. J. C. (1992): 'Two integrating sphere with an intervening scattering sample', *J. Opt. Soc. Am.*, **9**, pp. 621–631

SCHMIDT, M. H., MEYER, G. A., REICHERT, K. W., CHENG, J., KROUWER, H. G., OZKER, K., and WHELAN, H. T. (2004): 'Evaluation of photodynamic therapy near functional brain tissue in patients with recurrent brain tumors', *J. Neurooncol*, **67**, pp. 201–207

SCHROETER, M. L., BUCHELER, M. M., MULLER, K., ULUDAG, K., OBRIG, H., LOHMANN, G., TITTGEMEYER, M., VILLRINGER, A., and VON CRAMON, D. Y. (2004): 'Towards a standard analysis for functional near-infrared imaging', *Neuroimage*, **21**, pp. 283–290

STYLLI, S. S., HOWES, M., MACGREGOR, L., RAJENDRA, P., and KAYE, A. H. (2004): 'Photodynamic therapy of brain tumours: evaluation of porphyrin uptake versus clinical outcome', *J Clin. Neurosci.*, **11**, pp. 584–596

SWARTLING, J., DAM, J. S., and ANDERSSON-ENGELS, S. (2003a): 'Comparison of spatially and temporally resolved diffuse-reflectance measurement systems for determination of biomedical optical properties', *Appl. Opt.*, **42**, pp. 4612–4620

SWARTLING, J., PÅLSSON, S., PLATONOV, P., OLSSON, S. B., and ANDERSSON-ENGELS, S. (2003b): 'Changes in tissue optical properties due to radio frequency ablation of myocardium', *Med. Biol. Eng. Comput.*, **41**, pp. 403–409

VAN STAVEREN, H. J., MOES, C. J. M., VAN MARLE, J., PRAHL, S. A., and VAN GEMERT, M. J. C. (1991): 'Light scattering in Intralipid-10% in the wavelength range of 400–1100 nm', *Appl. Opt.*, **30**, pp. 4507–4514

WANG, L., and JACQUES, S. L. (1992): Monte Carlo modeling of light transport in multi-layered tissues in standard C: Laser Biology Research Laboratory, M. D. Anderson Cancer Center, University of Texas, Houston, Texas

WÅRDELL, K., ANTONSSON, J., and ERIKSSON, O. (2004): 'Optical measurements during experimental stereotactic neurosurgery'. International Federation for Medical & Biological Engineering (IFMBE), Ischia, Naples, Italy

WELCH, A. J., and VAN GEMERT, M. J. C. (1995): 'Optical-thermal response of laser-irradiated tissue' (Plenum Press, New York, 1995)

WILSON, B. C., JEEVES, W. P., and LOWE, D. M. (1985): '*In vivo* and *post mortem* measurements of the attenuation spectra of light in mammalian tissues', *Photochem. Photobiol.*, **42**, pp. 153–162

WOLF, M., WOLF, U., CHOI, J. H., TORONOV, V., PAUNESCU, L. A., MICHALOS, A., and GRATTON, E. (2003): 'Fast cerebral functional signal in the 100-ms range detected in the visual cortex by frequency-domain near-infrared spectrophotometry', *Psychophysiology*, **40**, pp. 521–528

YAROSLAVSKY, A. N., SCHULZE, P. C., YAROSLAVSKY, I. V., SCHOBER, R., ULRICH, F., and SCHWARZMAIER, H. J. (2002): 'Optical properties of selected native and coagulated human brain tissues in vitro in the visible and near infrared spectral range', *Phys. Med. Biol.*, **47**, pp. 2059–2073

Authors' biographies

NAZILA YAVARI received the MSc from University of Bergen, Norway. She has performed part of the research for her PhD program at Lund Institute of Technology, Medical Physics Group, Sweden. She is also a member of Lund University Medical Laser Centre. Her research interests include tissue optics, optical diagnostic methods and photodynamic therapy.

JAN S. DAM is currently working as a postdoc at the National Laser Centre, CSIR, in Pretoria, South Africa. His activities include absorption and scattering spectroscopy, light propagation modelling and multivariate data analysis. In 2000, he obtained his PhD in Biomedical Optics from Lund University, Sweden.

JOHAN ANTONSSON, MSc, and KARIN WÅRDELL, MSc, PhD and Professor of Biomedical Engineering, are working at Linköping University, Department of Biomedical Engineering. The research interests in their group include laser Doppler technology, reflection spectroscopy and RF technology with applications in stereotactic and functional neurosurgery.

STEFAN ANDERSSON-ENGELS, MSc, PhD, has been a Professor of Physics at Lund Institute of Technology since 1999. He is also strongly affiliated with the Lund University Medical Laser Centre, presently being the Head of the Board. His research interests include optical diagnostic methods in medicine, such as fluorescence and diffuse remission spectroscopy, as well as photodynamic therapy.